ARMY RESEARCH LABORATORY

Cationic Polymerization (Cure Kinetics) of Model Epoxide Systems

by Reza Dabestani, Ilia N. Ivanov, and James M. Sands

ARL-TR-2714

April 2002

Army Research Laboratory
Aberdeen Proving Ground, MD 21005-5069

ARL-TR-2714 **April 2002**

Cationic Polymerization (Cure Kinetics) of Model Epoxide Systems

Reza Dabestani and Ilia N. Ivanov
Oak Ridge National Laboratory

James M. Sands
Weapons and Materials Research Directorate, ARL

Abstract

Cationic polymerization of epoxy resins can be induced by ultraviolet (UV) or electron beam (E-beam) radiation and proceeds very efficiently in the presence of an appropriate photoinitiator. Although good thermal properties have been obtained for some E-beam cured epoxy resins, other important mechanical properties, such as interlaminar shear strength, fracture toughness, and compression are poor and do not meet aerospace manufacturers materials standards. We have initiated a comprehensive study to investigate the cure kinetics and mechanisms of UV and E-beam cured cationic polymerization of two epoxide-terminated resins (phenyl glycidyl ether, a monofunctional model compound, and Tactix 123, a difunctional structural resin) cured using a mixed triaryl iodonium hexafluoroantimonate salt (Sartomer's CD-1012) photoinitiator. The objective of this study was to demonstrate that identical reaction conditions and kinetic parameters (e.g., radiation dose, initiator concentration, and reaction temperature) control the physical and chemical properties of final polymeric products, regardless of initiation by UV or E-beam radiation. Additionally, the identification of key parameters that give rise to improved thermal and mechanical properties in E-beam processed resins is sought. Fast kinetic spectroscopy, coupled with high-performance liquid chromatography, was used to elucidate the polymerization mechanism and to identify the reactive intermediates, or molecules, involved in the cure process.

Acknowledgments

This research was partially supported through a Laboratory Directed Research Development Award administered by Oak Ridge National Laboratory. Oak Ridge National Laboratory is operated and managed by University of Tennessee-Battelle, Limited Liability Company for the U.S. Department of Energy under contract number DE-AC05-00OR22725. Additional support was provided by the U.S. Department of Defense through the Strategic Environmental Research and Development Program, under program PP-1109, "Non-Polluting Composites Repair and Remanufacturing for Military Applications."

INTENTIONALLY LEFT BLANK.

Contents

List of Figures

List of Tables

INTENTIONALLY LEFT BLANK.

1. Introduction

Currently, there is considerable interest in developing high-strength, lightweight polymer matrix composite materials for the aerospace and automotive industries. One class of resins that have the proper thermal and mechanical properties for these applications is toughened epoxies. These materials are typically processed by thermal (i.e., autoclave) curing methods, but recently, composites with comparable thermal and mechanical properties have been prepared by radiation curing. Ultraviolet (UV) and electron beam (E-beam) curing of resins and composites has received considerable attention in recent years [1-6]. Radiation curing typically uses high-energy radiation from an electron gun to induce polymerization and cross-linking reactions. E-beam curing is of great interest to industry because it has many advantages over thermal-curing methods that include lower cost, improved polymer performance, reduced energy consumption, lower residual thermal stress, reduced volatile toxic by-products, and simpler, less expensive tooling. E-beam processing is currently used for curing thin films for can and beverage coatings, printing inks for folding cartons, and anticorrosion coatings for automobile wheels [7]. Recent advances in E-beam curing of polymers has invoked onium salt promoters in cationic polymerization of vinyl ether monomers [8] and epoxy resins [9].

A fundamental understanding of the chemical events that lead to the desired material properties as well as a knowledge of the materials that undergo these radiation-induced reactions can provide researchers with the insight needed to control properties of the end products and to make advances into the development of novel resin systems for use in composites and adhesive applications. However, there is a lack of understanding concerning the chemical reactions that occur in the radiation curing of polymeric materials and the chemical structures that produce the desired mechanical properties. The goal of this study is to identify and optimize the parameters that control the material properties to facilitate preparation of new composites with advanced mechanical and thermal properties from epoxy resins by radiation curing.

2. Background

Radiation induced cationic polymerization in the presence of an initiator has not been investigated in detail. A plausible mechanism for radiation curing of epoxy resins by cationic polymerization in the presence of onium salts has been

proposed recently to explain the curing process [9]. The assigned intermediates, however, are speculative (not based on experimental evidence), and their rates of reaction to form cross-linked and/or scission products are unknown (Figure 1) [9]. Thus, a basic understanding of the kinetics and mechanisms of radiation curing leading to crosslinking and scission (an undesirable process that can adversely affect the properties of final composite) products is needed to set the criteria for developing application-specific composites.

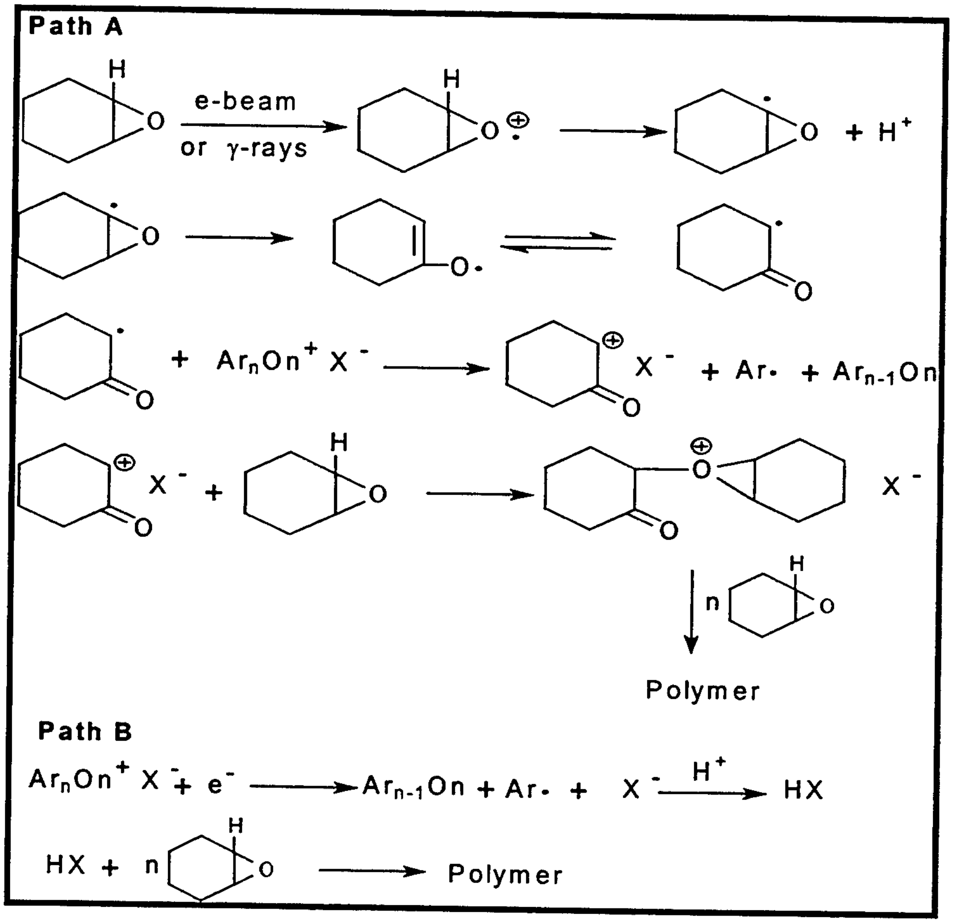

Figure 1. Proposed reaction mechanism for cationic ring-opening of epoxides using E-beam initiation.

We have taken a fundamental approach to investigate the chemistry of radiation curing of phenyl glycidyl ether (PGE) and Tactix 123 as model compounds in the presence of a mixed triaryl iodonium hexafluoroantimonate salt (Sartomer's CD-1012) as the photoinitiator. Insight gained from these experiments should pave the way towards the design and synthesis of novel composites, which will be of significant interest to the defense, aerospace, and transportation industries.

3. Experimental

3.1 Materials

The structure of all the reagents used in this study are shown in Figure 2. All the solvents used were high-performance liquid chromatography (HPLC) grade and include tetrahydrofuran (THF), acetonitrile (ACN), and water. Bromophenol blue (3',3'',5',5''-tetrabromophenolsulfonephthalein) was used as received from Aldrich Chemical Company. Gel permeation chromatography (GPC) was performed on a Waters 600E Instrument. HPLC analysis of the samples was carried out under isocratic conditions (75/25 acetonitrile/water) using a Hewlett Packard Model 1090 equipped with a diode array detector set at 254 nm. Absorption spectra of the samples were obtained on a Cary 4 spectrophotometer. Fast kinetic studies using pulse radiolysis were conducted at Notre Dame Radiation Facilities, University of Notre Dame, Notre Dame, IN.

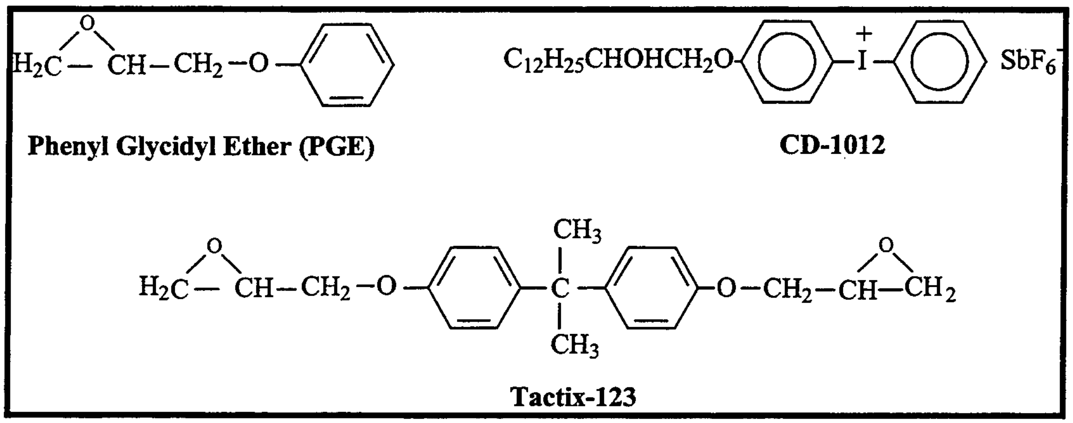

Figure 2. Structures of reagents used to evaluate chemical kinetics.

3.2 Procedure

3.2.1 Sample Preparation and UV-Photolysis

Our initial kinetic studies on UV cationic polymerization of Tactix 123 in the presence of CD-1012 focused on polymerization rate and the nature of polymeric materials formed. Tactix 123 samples were prepared containing 3% by weight CD-1012 in glass tubes (~1 g total weight) and photolyzed in a Rayonet photoreactor using 300-nm excitation light source. After the photolysis, a known volume of THF was added to the irradiated sample to dissolve the low molecular weight polymers, and the mixture was filtered leaving an insoluble material (cross-linked polymer) which was dried and weighed. A portion of the THF

mixture was analyzed by HPLC to determine the loss of Tactix 123 by irradiation. The remaining THF solution was concentrated down and analyzed by GPC to obtain information on low molecular weight polymers formed during photolysis.

3.2.2 Pulse Radiolysis

Time-resolved studies of the intermediates were performed using pulse radiolysis, where excitation was induced using a linear electron accelerator (Model TBS-8/16-1sTitan Beta, Dublin, CA) that generates 1- to 10-ns pulses of 8 MeV. These pulses were used as the excitation source and were delivered to a flow cell containing the sample. Intermediates generated by the electron pulse were detected by optical absorption using a pulsed 1-kW Xe-lamp (samples were in quartz cuvette with a optical path length of 1 cm). All experiments were carried out with a continuously flowing solution. A solution of potassium thiocyanate (10 mM) saturated with nitrous oxide was used as the dosimeter (using radiation chemical yield of 6.13 for a dimer of cyanide anion $(SCN)^{-}_{2}$ and a molar coefficient of 7580 $M^{-1}cm^{-1}$ at 472 nm). The data acquisition system included a Spex 270M monochromator, a LeCroy 7200A digital storage oscilloscope with a 7242 plug-in module and a shielded 5-stage photo-multiplier tube (PMT, Hamamatsu 955). Software program with incorporated multiple time scale stages, developed by G. L. Hug, was used for running the pulse radiolysis experiment [10].

3.2.3 Steady State Radiolysis

Steady state gamma radiolyis studies were performed on two programmable cobalt-60 gamma irradiators with radiation intensities of about 2 and 6 kilo Curies and dose rates of 5 and 20 krad/min, respectively. Samples were placed in capped glass vials. Insignificant increase in the temperature of the sample was observed when the sample was irradiated for a long period of time. After irradiation, samples were analyzed by optical absorption spectroscopy.

4. Results and Discussion

4.1 UV Photolysis of Tactix 123 Containing 3% (Weight) CD-1012

Table 1 shows the data for a set of samples irradiated at various times. As the data in Table 1 shows, the yield of insoluble polymer (crosslinked material) increases with increasing irradiation time and accounts for about 70% of the total polymer formed. Samples irradiated to >90% conversion of Tactix 123 completely solidified and were hard to remove from the glass tube by THF.

Table 1. HPLC and GPC analysis data for the photolysis (300 nm) of Tactix 123 in the presence of CD-1012 as the photoinitiator.

Irradiation Time (min)	Moles Tactix at Time 0	Moles Tactix After Irrad.	% Loss [a] Tactix	% Polymeric Cross-Linked Insoluble Product [b]	%Polymeric Soluble Products[c]
3	2.4 E-3	2.2 E-3	8.8	0.0	100
6	2.6 E-3	2.1 E-3	20.9	19.0	81.0
9	3.1 E-3	1.7 E-3	47.7	22.0	78.0
12	3.0 E-3	1.7 E-3	43.7	56.0	44.0
18	2.8 E-3	1.1 E-3	60.4	67.0	33.0
24	2.7 E-3	9.7 E-4	64.1	69.0	31.0

[a] Data obtained by HPLC.

[b] Percent crosslinked insoluble polymeric product in THF (based on weight).

[c] Percent soluble product based on GPC analysis of dissolved fraction in THF. Three broad peaks eluting at 19, 21, and 24 min (unreacted CD-1012 and Tactix 123 elute at 26 and 29 min, respectively).

As a result, the exact weight of insoluble polymer could not be determined for high-conversion samples. Figure 3 shows a plot of percent loss of Tactix 123 monomer as a function of irradiation time for the data shown in Table 1.

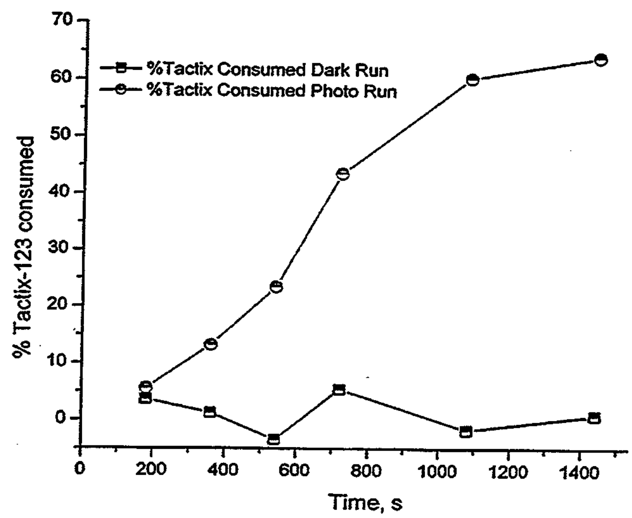

Figure 3. Percent loss of Tactix 123 monomer as a function of irradiation time.

From the plot of 1n (A/A_0) vs. irradiation time (not shown), the first-order rate constant for loss of Tactix 123 was determined to be $k = 7.6 \times 10^{-4}\ s^{-1}$. During the course of photolysis, a small increase in temperature rise was observed. To study the effect of this temperature rise on the reaction rate, we prepared two samples of Tactix 123 without CD-1012 (set A) and two samples of Tactix 123

with CD-1012 (set B). In one experiment, one sample of set A and one of B were placed in a water bath at 25 °C. A thermocouple was placed inside each reaction mixture to monitor the temperature change during irradiation. Sample B was irradiated for a total of 240 s, while sample A was irradiated for 500 s. The rise in temperature as a function of irradiation time was recorded for both materials (Figure 4), and the loss of Tactix 123 monomer was determined by HPLC for each irradiated sample.

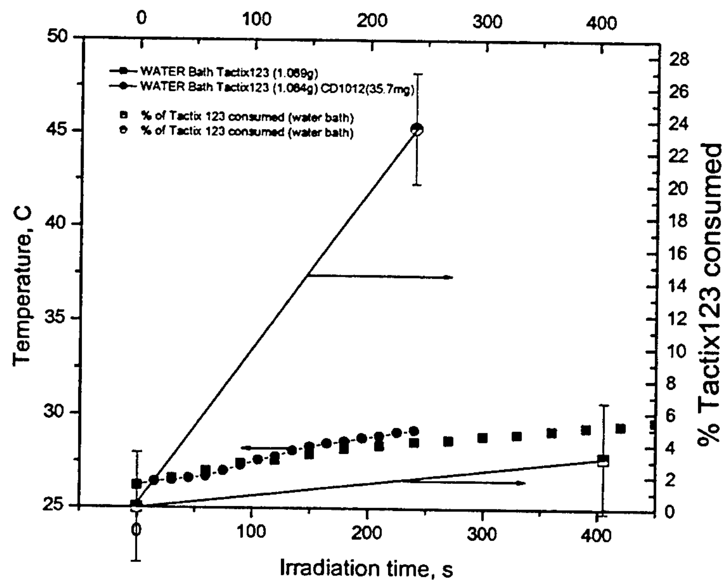

Figure 4. Rise in temperature as a function of irradiation time for Tactix 123 with CD-1012 and without CD-1012.

Because Tactix 123 without CD-1012 does not react, as demonstrated in Figure 3, the observed variance (±5%) is the expected experimental error using the HPLC method of postirradiation analysis. Tactix 123 containing CD-1012 lost about 26% ± 5% in 600 s. The rise in temperature during irradiation for Tactix without CD-1012 was about 3 °C, which we attribute to lamp heating. For Tactix 123 with CD-1012, about 5 °C (Figure 4) rise in temperature was observed. Taking into account the 3 °C rise in temperature due to lamp heating, the rise in temperature as a result of bond breaking (internal temperature rise) during the reaction is only +2 °C. Therefore, we believe that the water bath and small sample size essentially allow for isothermal cure conditions to be maintained.

The same experiment was carried out for the second set of samples in air, allowing heat of reaction to cause appreciable changes in temperature. The results are shown in Figure 5. Observed temperature and extent of Tactix 123 conversion are plotted as a function of irradiation time. The rise in temperature during irradiation for the set A sample was +10 °C, and because no reaction occurs, this is attributed to thermal absorption from the UV excitation lamp. For

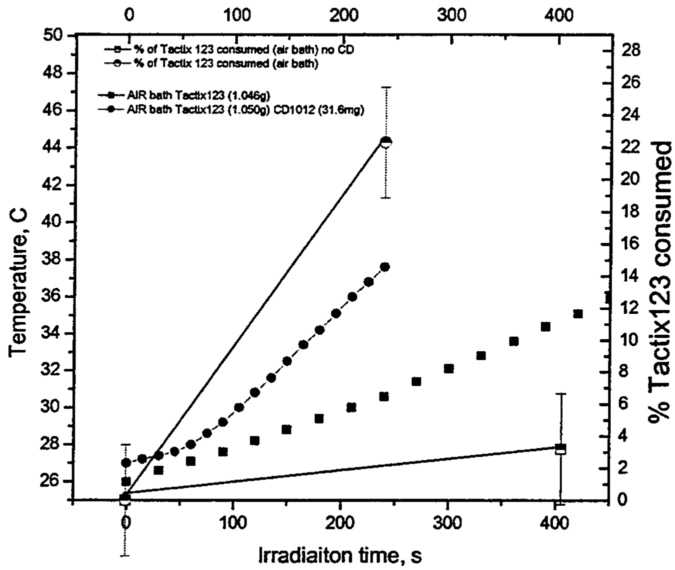

Figure 5. Observed temperature and extent of Tactix 123 conversion.

the set B sample, the temperature rise was +21 °C, or a reaction temperature induced change of +11 °C, resulting from breaking chemical bonds. THF extraction and HPLC analysis of the irradiated sample showed a 23% ±5% conversion of Tactix 123 in 240 s (Figure 5). Comparison of the results for water bath vs. atmospheric irradiation demonstrate that within experimental detection limits, the internal rise in temperature induced during photolysis does not lead to a rate enhancement during photolysis measurements.

The effect of external temperature on the reaction rate was also studied for samples of Tactix 123 with CD-1012 to obtain the activation energy, E_a, and the Arrhenius A-factor for the polymerization process. Figure 6 shows the Arrhenius plot for the change in rate constant as a function of inverse temperature for the photolysis of Tactix 123 with CD-1012. From the slope and intercept of this plot, we obtain an activation energy of 61 kJ/mol and an Arrhenius-A factor of 2.4×10^8 s^{-1}. The observed deviation of reaction rate at higher temperatures (T > 60 °C) could be due to faster molecular diffusion that could facilitate recombination of reactive species back to starting material.

According to Figure 1, polymerization of the epoxy resins proceeds by the interaction of electrons with the monomer (path A) or photoinitiator (path B). In order to determine the extent to which each path (if any) contributes to the polymerization process, we carried out pulse radiolysis experiments on PGE (a model compound that upon polymerization forms soluble products), CD-1012, and PGE/CD-1012 mixtures to obtain information on the nature of intermediates produced in each case.

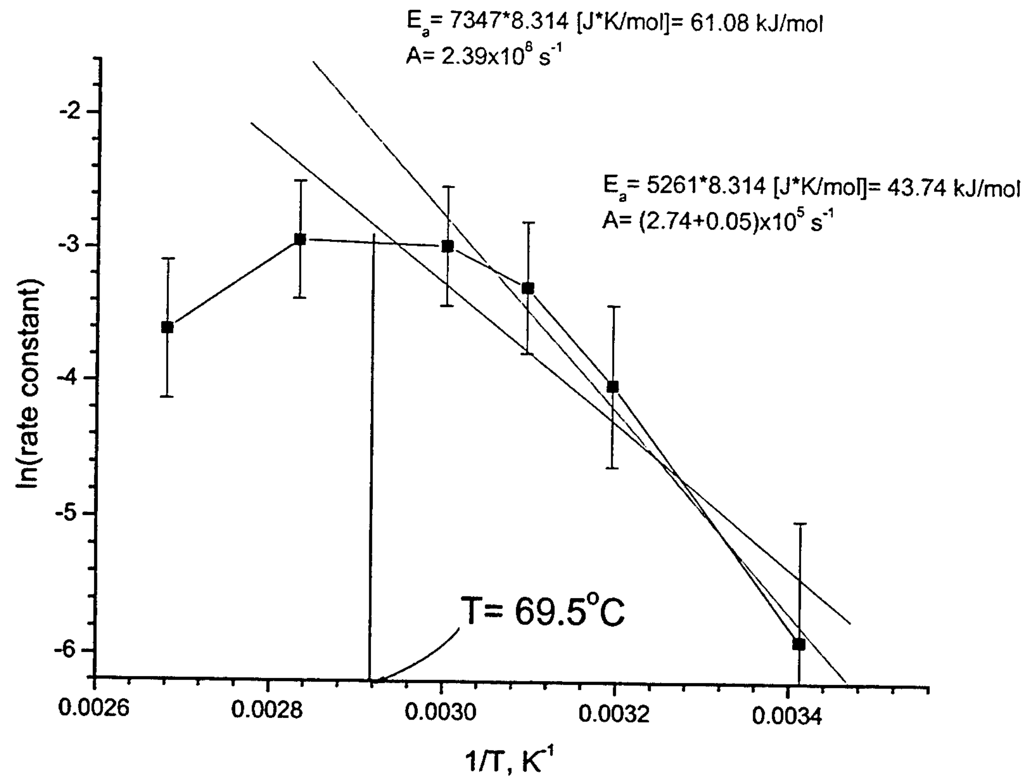

Figure 6. Change in rate constant as a function of inverse temperature for the photolysis of Tactix 123 with CD-1012.

4.2 Steady State γ-Radiolysis

Radiolysis of CD-1012 in aerated acetonitrile was monitored directly by following changes in the absorption spectrum of the solution using nonirradiated acetonitrile as a reference. At low dose rates (5 krad/min), changes in the absorption spectrum of CD-1012 indicate the presence of two isosbestic points observed at 309 nm and 351 nm (Figure 7). As the absorbed dose increases, the absorption in the 200- to 250-nm region of the spectrum increases concomitant with a decrease in the 300- to 400-nm wavelength region. At higher dose rates (20 krad/min), no isosbestic points are observed, and an overall increase in the absorbance is observed (Figure 8). Changes in the intensity of the 234-nm absorption band for CD-1012 with time, upon steady state γ-radiolysis of 70-μM solution of CD-1012 in aerated acetonitrile for two different dose rates (5 and 20 krad/min), is shown in Figure 9. It can be seen from Figure 9 that high dose rates significantly increase the rate of growth for the 234-nm band compared to low dose rates. The 234-nm absorbance almost doubled after exposing the solution for 25 min at 20 krad/min dose rate, while irradiation for 115 min at lower dose rate (5 krad/min) resulted in *ca.* 72%

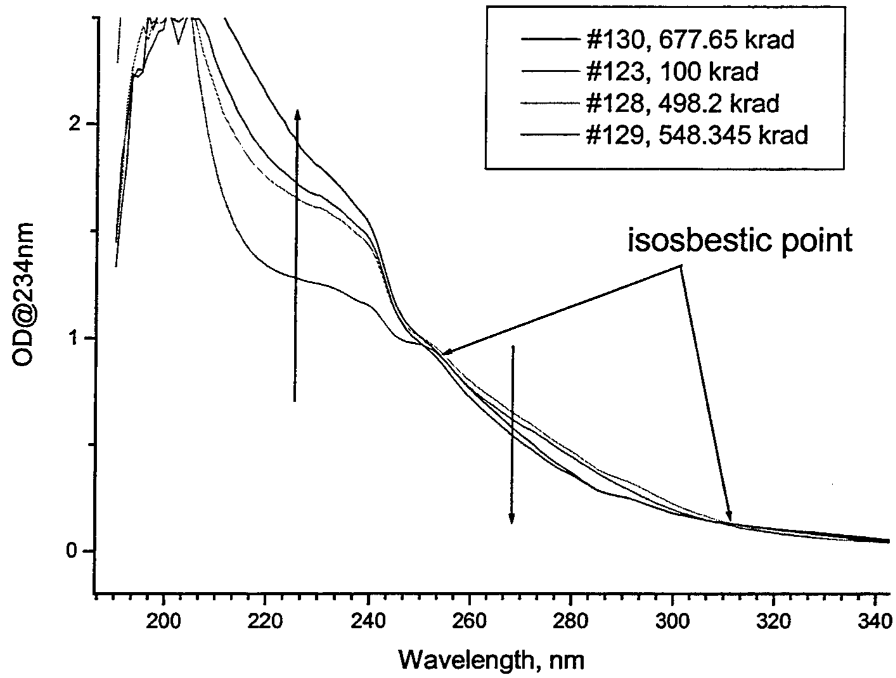

Figure 7. Changes in the UV-Vis absorption spectrum of CD-1012 (70 μmol/L) in aerated acetonitrile observed upon γ-radiolysis (5 krad/min dose rate).

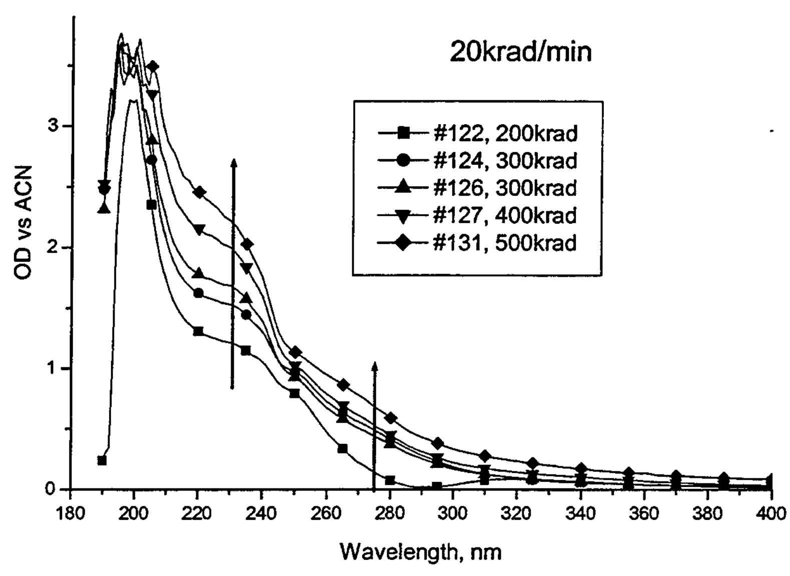

Figure 8. Changes in the UV-Vis absorption spectrum of CD-1012 (70 μmol/L) in aerated acetonitrile observed upon γ-radiolysis (20-krad/min dose rate).

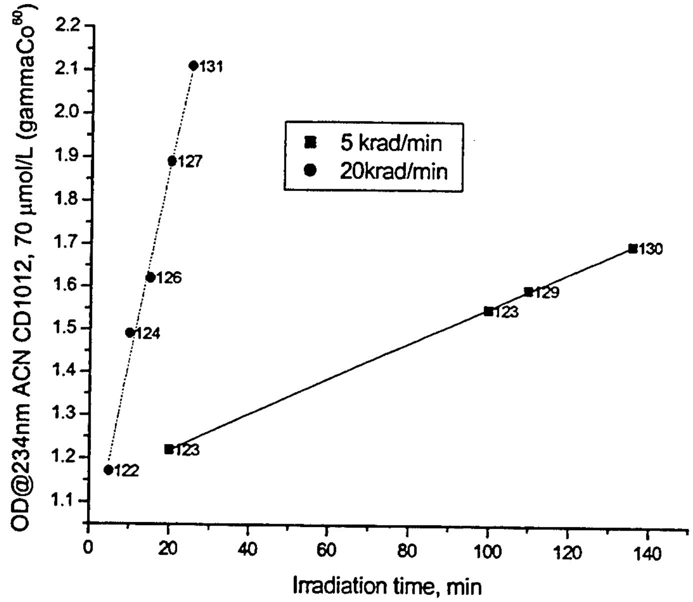

Figure 9. Changes in the intensity of 234-nm absorption band of CD-1012 (aerated 70-µM solution in acetonitrile) with time upon steady state γ-radiolysis (dose rates: 5 and 20 krad/min).

increase in the absorbance. The difference in the rates of growth for 234-nm band under high and low dose rates is a factor of 116, which is much greater than the factor of 4 increase in dose rate. If the observed changes in UV-Vis region of the spectrum are due to formation of the same species (e.g., a precursor to superacid), then at high dose rates, one should produce much more superacid according to the sequence of the reactions shown in Figure 2.

Formation of superacid was monitored by adding bromophenol blue indicator to the irradiated samples of CD-1012. In order to avoid interference from bromophenol blue radiation chemistry with that of CD-1012, the indicator was added after irradiation to a diluted solution of CD-1012 in acetonitrile. An increase in the acidity of the media should result in a decrease in the intensity of the 595-nm absorption band of the bromophenol blue indicator. The change in bromophenol blue absorbance at 595 nm caused by a decrease in the pH of the mixture as a result of radiolytic decomposition of CD-1012 is shown in Figure 10. The data confirms the formation of protons by CD-1012 radiolysis. For high dose rates (20 krad/min), the decrease in the 595-nm absorbance is smaller (almost by a factor of 2) than that for the low dose rate. One possible explanation for this observation is that the yield of superacid precursor (solvent-SbF_6 ion pair or SbF_6^-) decreases at a high dose rate. A decrease in superacid precursor is likely, provided recombination reactions lead to the formation of an intermediate incapable of generating superacid. The changes in the 595-nm absorption appears to be insensitive to the dose rate.

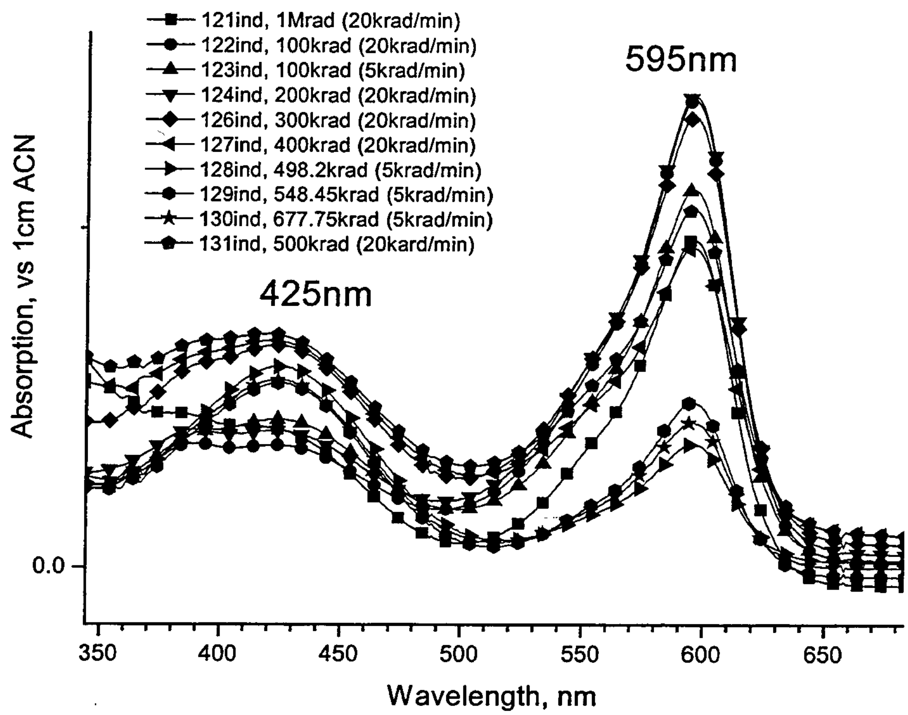

Figure 10. Changes in the UV-Vis absorption spectra of bromophenol blue (35 μmol/L) added to an irradiated (5 and 20 krad/min, blue and black curves) solution of CD-1012 (70 μmol/g) in aerated acetonitrile.

4.3 Pulse Radiolysis of Degassed PGE

Decay of the transient absorption spectrum obtained upon pulse radiolysis of degassed PGE is shown in Figure 11. The transient spectrum observed 0.5 μs after the electron pulse exhibits peaks at 300, 333 (sh), and 400 nm. The 333-nm absorption is buried under the intense 300-nm band and appears at 0.5 μs after the pulse as a shoulder. A broader band with intensity much smaller than that of 300 nm is observed in the 400- to 500-nm wavelength region. The transient spectrum changes significantly 3.0 μs after the pulse. Most of the spectral features, however, resemble the spectrum observed at 0.5 μs after the pulse, except for a broad band. At longer times (>50 μs), the transient spectrum does not change significantly. On the basis of the observed transient spectra, it is clear that the major absorption band (300 nm) corresponds to the first intermediate formed and the broad bands at 400 nm and higher to a second intermediate. Assuming that the spectral features of LLI are the same throughout the observed time scale and that the 300-nm absorption band is mostly due to this species, we can deduce the spectral features of the second

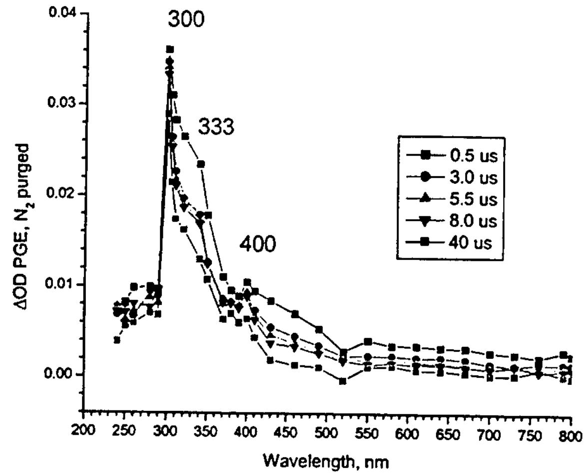

Figure 11. Transient absorption spectrum of nitrogen saturated PGE obtained at 0.5, 3.0, 5.5, 8.0, and 40 μs after the pulse.

intermediate by subtracting the normalized spectrum obtained at 160 μs after the pulse from the normalized spectrum obtained at 0.5 μs after the pulse (both spectra normalized at 300 nm) (Figure 12). The subtracted spectrum representing the second intermediate exhibits absorption bands at 310, 340, and 430 nm, respectively. The complex nature of this transient can be seen in Figure 13, with time profiles of optical density monitored at the major absorption bands 300, 340, 400, and 430 nm. Thus, the 300-nm absorbance attributed to the first intermediate appears to be within the pulse duration (10 ns) of our instrument and continues to grow with a lifetime (τ) of 1.56 ± 0.27 μs (nonlinear least squares fitting procedures with Levenberg-Marquardt algorithm was used). Continuous formation of the 300-nm absorption due to first intermediate appears to be concomitant with the decay of the 430-nm band of second intermediate. The decay profiles could not be fitted to a mono-exponential equation, suggesting the presence of more than one component in these transients. Two-exponential fit of 430-nm decay gave two lifetimes of 4.88 ± 0.45 μs and 60.0 ± 3.4 μs (indicative of the presence of two components), respectively. Decay of the 300-nm absorption band, using the two-exponential model, gave two lifetimes of 3.62 ± 0.79 and 70.0 $\pm$ 1.1 μs (also suggesting the presence of two components in this intermediate), respectively. If the first lifetime of the 430-nm band (second intermediate) is kept constant at 3.62 μs, the second component lifetime is estimated to be 60.0 ± 0.8 μs. When the second component lifetime of 430-nm intermediate is restricted to 70 μs, the first component lifetime of 8.19 ± 0.52 μs is obtained. Because the first and second intermediates were observed right after the excitation pulse, it is reasonable to assume that their precursor is either a PGE cation radical or solvated electron (*vida infra*).

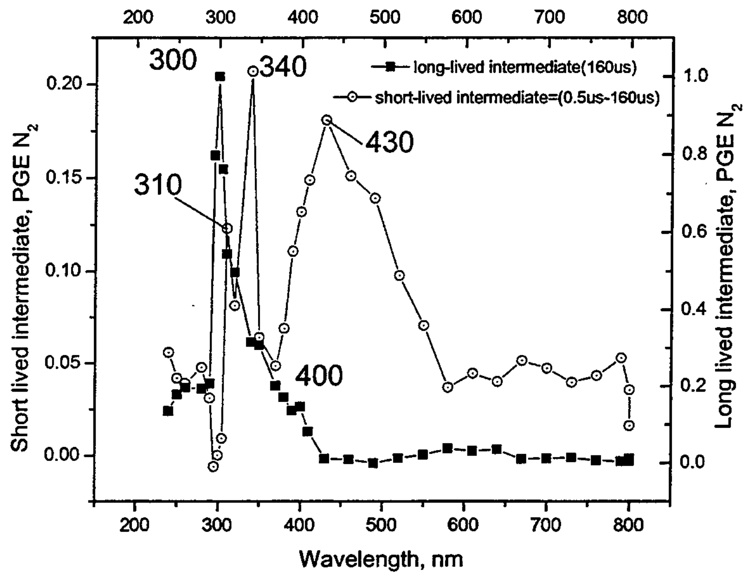

Figure 12. Transient absorption spectra of short-lived and long-lived intermediates obtained upon pulse radiolysis of PGE. The spectrum of the short-lived intermediate was determined by subtracting the spectrum of the long-lived intermediate (taken 160 μs after the pulse) from the spectrum obtained at 0.5 μs after the pulse.

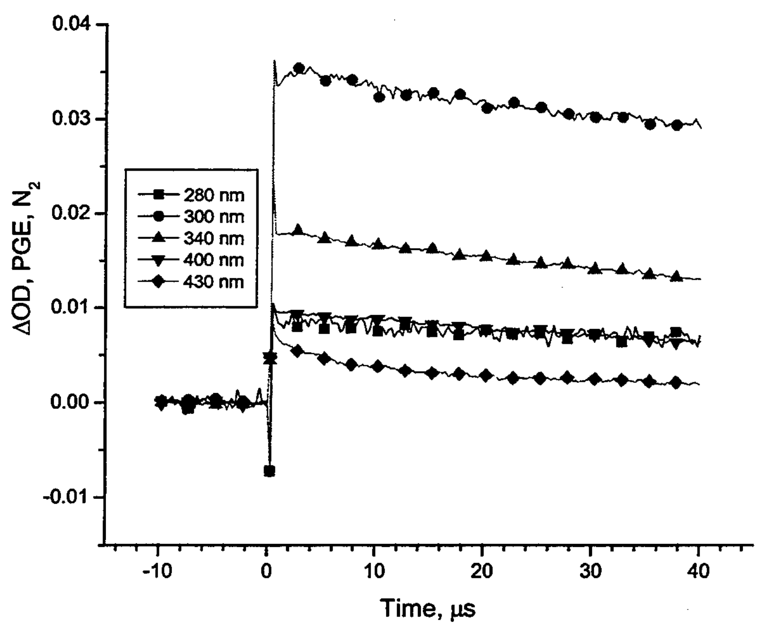

Figure 13. Changes in the optical density at major absorption bands (280, 300, 340, 400, and 430 nm) obtained upon pulse radiolysis of degassed PGE.

4.4 Pulse Radiolysis of Oxygenated PGE

The major absorption bands in the transient absorption spectrum of oxygenated PGE obtained 0.5 μs after the pulse are similar to those found for degassed PGE (300, 340 [sh], 400 and 425 nm) (Figure 14). A decrease (factor of 1.5) in the initial intensity of the 340-nm absorption band is observed compared to degassed PGE. This shoulder was previously attributed to the spectral signature of a second intermediate. Oxygen does not quench SLI completely, and similar to degassed PGE, we observe a significant difference between the 0.5- and 3.0-μs spectra indicative of the presence of this intermediate. The spectrum of this intermediate shows features that are quite similar to that observed in degassed PGE with the major absorption bands at 310, 340, and 425 nm. The difference between these spectra is in the relative band intensities. Oxygen appears to quench the 340-nm band of this intermediate, as well as the narrow band at 430 nm. This observation, coupled with the fact that oxygen does not affect the spectral features of the first intermediate (300-nm band), suggests that the second intermediate has a complex nature and that its spectrum consists of at least two components (with different sensitivity to oxygen). The absorption band at 340 nm belongs to the oxygen-sensitive, short-lived component, while the oxygen-sensitive component shows a broad absorption band at 425 nm. A 5-nm blue shift in the position of the 430-nm absorption band in the oxygen-purged PGE compared to the degassed sample could be due to significant overlap of the absorption spectra of for these two components in the absence of oxygen. All the intermediates are formed right after the pulse. Kinetic profiles do not show additional rise in the 300-nm absorption band for the first intermediate at the expense of the 425-nm band of the second intermediate. This suggests that the oxygen-sensitive component of the second intermediate is a plausible precursor for additional formation of the first intermediate in deoxygenated PGE.

4.5 Pulse Radiolysis of N_2O Saturated PGE

In N_2O saturated PGE, solvated electrons can interact with N_2O to produce hydroxy radicals according to equation (1):

$$\bar{e}_{solv} + N_2O + PGE \rightarrow N_2 + OH^{\bullet} + OH^{-}. \qquad (1)$$

Hydroxy radicals could potentially attack the ether or epoxy group of the PGE, causing a change in the UV-Vis absorption spectrum of intermediates. The transient absorption spectrum of PGE saturated with nitrous oxide measured at 0.5, 3.0, 5.5, 8.0, and 40 μs after the electron pulse is shown in Figure 15. Spectral features and relative band intensities are similar to the transient absorption spectrum of degassed PGE with the maxima at 300, 340(sh), 400, and 425 nm, and a broad absorption band in the 450- to 750-nm region. The spectrum of the second intermediate is deduced by subtracting the transient spectrum obtained 200 μs after the pulse from that obtained 0.5 μs after the pulse (both normalized

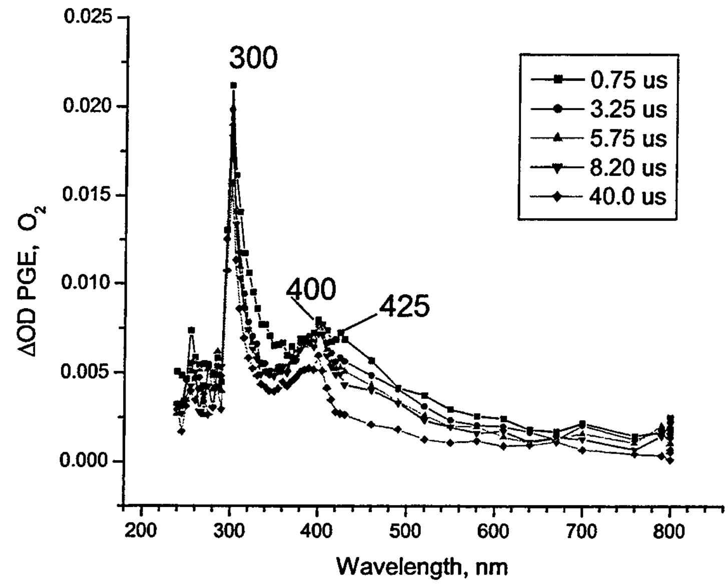

Figure 14. Transient absorption spectra of oxygen saturated PGE taken at 0.75, 3.25, 5.75, 8.20, and 40 μs after the pulse.

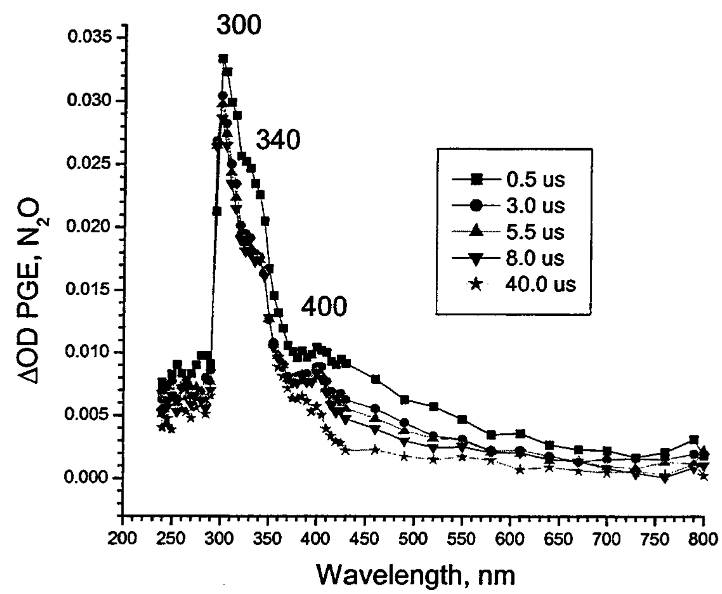

Figure 15. Transient absorption spectra of N_2O saturated PGE taken at 0.5, 3.0, 5.5, 8.0, and 40 μs after the pulse.

at 300 nm). The difference spectrum shows maxima at 330 and 425 nm and a shoulder at 520 nm. Relative intensity of the 330-nm absorption band (compared to that at 425 nm) in the spectrum of this intermediate falls between the values for degassed and oxygen-saturated solution. Similar to degassed PGE, the 300-nm kinetic shows a rise of absorbance within the first few microseconds after the pulse (0.75 ± 0.10 μs), followed by its decay, to give much longer lifetimes of 8.65 ± 0.95 and 90 ± 3.92 μs for its two components. The 425-nm absorbance decays to give a short component lifetime of 0.97 ± 0.11 μs (which is close to the risetime of the 300-nm absorbance) and a relatively slow second component with a lifetime of 70 μs. Similar to the deoxygenated PGE, post-pulse formation of the 300-nm absorbance takes place at the expense of the 425 nm band. The long-lived component of the 340-nm band decays with a lifetime of 70 μs, and the short-lived component decays with a lifetime of 1 μs. Most of the absorbance decays for the second intermediate shows a long-lived component with a lifetime of ca. 70 μs (limited to 200-μs time scale with a pulse-lamp). Based on these results, the range of lifetimes for the long-lived component is 70–90 μs.

4.6 Assignment of Intermediates

Figure 16 depicts plausible intermediates produced by pulse radiolysis of PGE, labeled (1) in that figure. We observe no changes in the initial yield of the intermediates in the presence of N_2O, suggesting that solvated electrons do not play a significant role in their production. Thus, a cation radical of PGE appears to be the most suitable precursor for the formation of all the intermediates observed in the 0- to 200-μs time scale with absorption in the range of 250–800 nm. A cation radical can form by either the ether oxygen or the epoxy oxygen of the PGE. The opening of the epoxy ring is more favorable (releasing 112 kJ of energy) than cleavage of an ether bond (25.3 vs. 44.0 kcal/mol). Therefore, the observed transients are most likely formed by this ring-opening process and can proceed by both paths shown in Figure 16. Loss of a secondary or tertiary proton on the carbon atom adjacent to the epoxide oxygen produces free radical species 4 and 4a. Cleavage of the carbon-oxygen bond is followed by the rearrangement of free radical species to give the resonance stabilized radicals 9, 10 and 9a, 10a. Resonance-stabilized intermediates 9, 10 and 9a, 10a could be assigned to the transient absorption of the first intermediate. Equilibration between the resonance forms of LLI appears to be so fast that we cannot distinguish between them under the conditions of our experiment. However, the presence of more than one lifetime, when fitting these transient absorbances, suggests that several species with relatively similar structures are present. Spectral features of the first intermediate (strong absorption at 300 nm and weaker absorption bands in the 400- to 500-nm wavelength region) agree well with the published spectral characteristics of aromatic ketyl radicals. This notion is further supported by the fact that oxygen does not quench these intermediates.

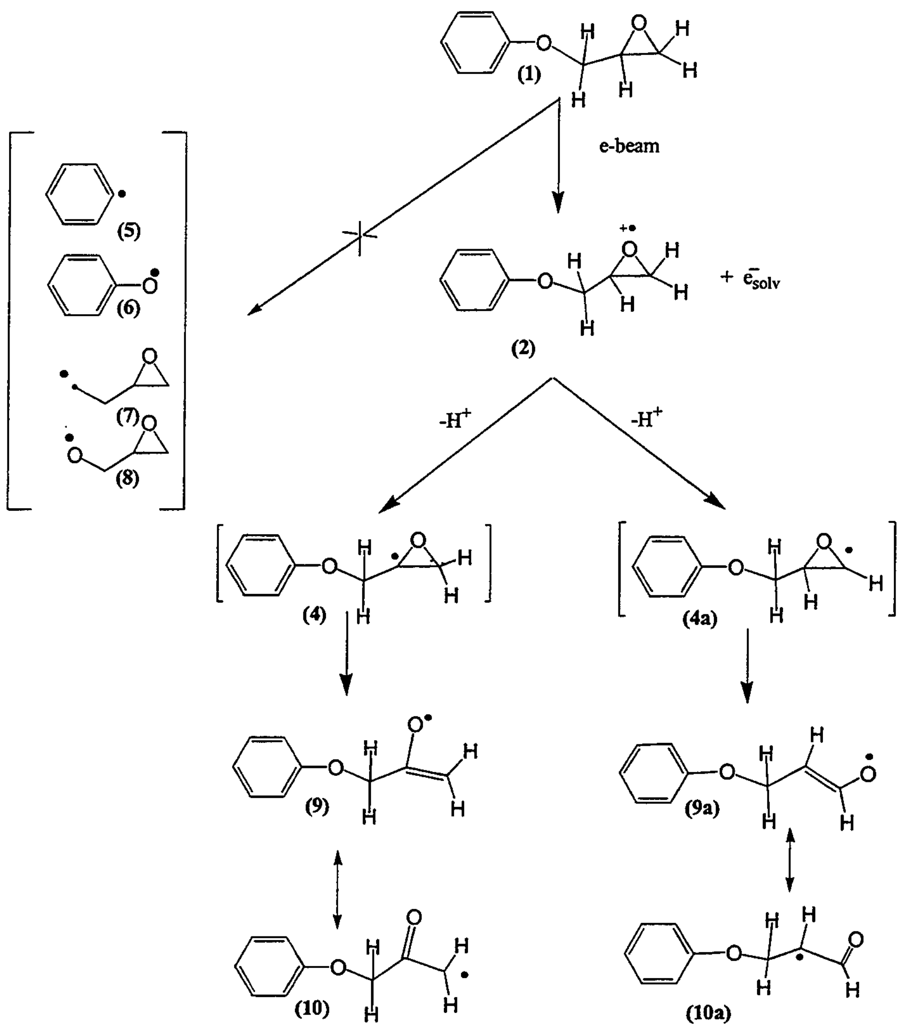

Figure 16. Plausible intermediates produced by pulse radiolysis of PGE.

Additional formation of this intermediate from the oxygen-sensitive component of the second intermediate is observed for all solutions, except for oxygen-saturated ones. Quenching of the oxygen-sensitive component of the second intermediate by oxygen suggests that it is a carbon-centered radical species (with no ketyl character). Intermediates 4 and 4a match these conditions for the oxygen-sensitive transient. The second short-lived component, which is not oxygen sensitive, absorbs at a longer wavelength than the oxygen-sensitive one and could form from the cleavage of epoxy ring. The fact that this component is not quenched by oxygen suggests that it is a zwitterionic species. Hence, intermediate 2 with its ionic character is a plausible candidate. The spectral features of the first and second intermediates, which absorb at a much longer wavelength than any of the possible radicals 5–8 shown in Figure 16, substantiate our proposed mechanism that the PGE ether linkage remains intact upon pulse

radiolysis. Radicals 5–8, which are derived from the homolytic cleavage of ether bond in PGE, where extended conjugation with the phenyl moiety is lost, will absorb at shorter wavelengths.

4.7 Pulse Radiolysis of Degassed PGE Containing 3% (Weight) CD-1012

The evolution and decay of the transient absorption spectrum of degassed PGE in the presence of 3 weight-percent CD-1012 is shown in Figures 17(a) and 17(b). The spectral features of the intermediate with maxima at 360 and 400 nm changes with time. Growth of the 400 nm absorbance maximizes in approximately 11 μs after the pulse and decays on a much longer time scale. Figure 17(b) shows that at longer times (>20 μs after the pulse), the 435-nm band becomes a major absorption band in the transient spectrum and decays on a much longer time scale. About one third of the transient spectrum decayed within 160 μs (limits of pulsed probe lamp). Similar spectral changes were also observed for the transient in the 500- to 800-nm wavelength region (not shown). This transient exhibits a maximum absorption at λ_{max} > 800 nm and two shoulders at 605 and 685 nm (not shown). Spectral features of these intermediates change with time. At 160 μs after the pulse, only the spectrum of transient with λ_{max} > 800 nm is still observed.

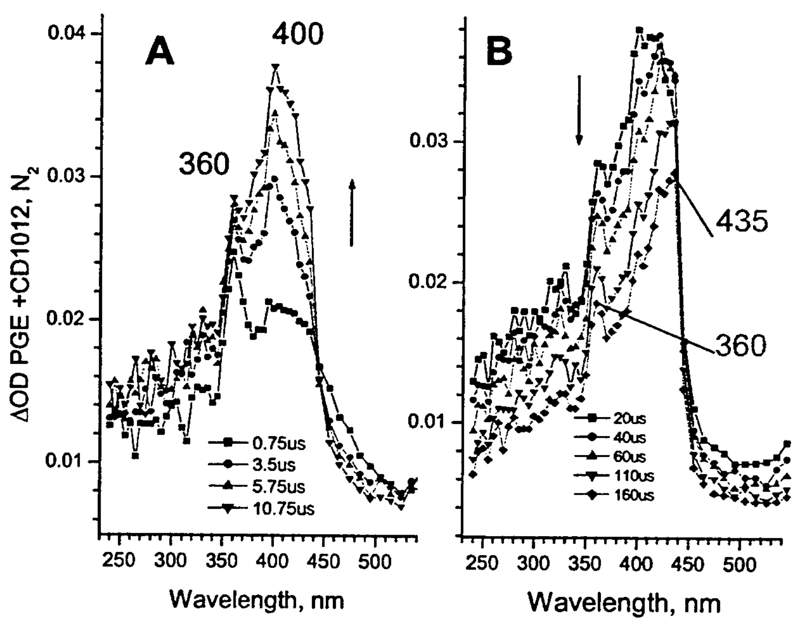

Figure 17. Transient absorption spectrum of degassed PGE in the presence of *ca.* 3% CD-1012 taken at (a) 0.75, 3.5, 5.75, and 10.75 μs and at (b) 20, 40, 60, 110, and 160 μs after the excitation pulse.

We observe significant variation in the risetime of transients (e.g., from 2 μs for 605-nm absorbance to 20 μs for 435-nm band). Almost all the absorption bands reach their maximum value between 20 and 60 μs after the pulse, suggesting that these transients are formed by secondary processes.

4.8 Tentative Assignment of Intermediates Observed on Pulse Radiolysis of Degassed PGE Containing 3% (Weight) CD-1012

None of the transients previously assigned to the first intermediate (9, 9a, 10, and 10a in Figure 16) were observed in the pulse radiolysis of PGE containing 3% CD-1012. Such observation suggests that at this concentration of CD-1012, all PGE intermediates are intercepted by CD-1012, leading to the observed transients. Additional intermediates are produced by the reduction of iodonium salt with solvated electrons (Figure 18). Products of this reaction are an aryl radical (13), hexafluoroantimonate anion (14), and an aryl iodide (12). A strong Brönsted acid, $HSbF_6$ (15), is also generated upon hydrogen abstraction from the PGE molecule by hexafluoroantimonate anion (14). The polymerization reaction shown in Figure 18 proceeds through the reduction of iodonium salt, Ar_2ISbF_6, by either radicals 9, 9a, 10, 10a in Figure 16, or by the solvated electrons producing the intermediates 11 and 11a. The products of this reaction are an aryl radical 13, hexafluoroantimonate anion 14, and an aryl iodide 12. The aryl radical 13 could abstract a hydrogen atom from a molecule of PGE 1 to produce intermediates 4 and 4a, which can proceed to form polymer according to the scheme in Figure 18. Alternatively, the acid-catalyzed ring-opening of the epoxy proceeds through intermediate 16, which has 14 as a counter ion. Ring-opening can take place to generate two different intermediates, 17 and 17a. Interaction of a PGE molecule with either 17 or 17a can produce intermediates 18 or 19, starting a repeating unit of polyphenylglycidyl ether (PPGE).

The observed absorption in the 300- to 600-nm region can be assigned to either intermediates 11 and 11a, or intermediates 17 and 17a with 14 as a counter ion. However, the fact that there is no significant absorbance in the 300-nm region, where ketyl intermediate absorbs, suggests that intermediate 17 is the most likely candidate. It also indicates that initiation of cationic polymerization by PGE radicals is not very efficient compared to polymerization initiated by the reaction of CD-1012 with solvated electrons. The broad absorption band around 605 nm could be attributed to the absorption of diaryliodonium radical cation based on the literature data. It is also plausible that the radiolysis of PGE in the presence of 3% CD-1012 does not proceed to give the first intermediate (9, 9a, 10, and 10a in Figure 16). The precursor of this intermediate, which is the oxygen-sensitive component of the second intermediate, reduces CD-1012, producing the same combination of intermediates 12, 13, and 14, as well as ring-opening of the epoxy ring without the formation of a ketyl intermediate. This is consistent with our experimental observation that the observed transient obtained at 0.75 μs after the

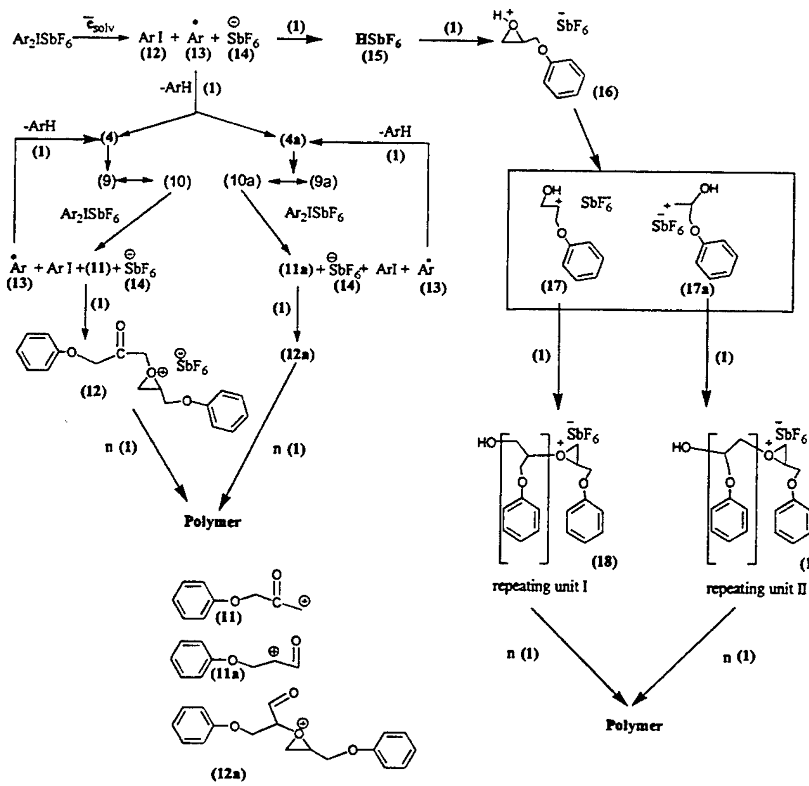

Figure 18. Plausible intermediates produced by pulse radiolysis of 3% CD-1012 in degassed PGE.

pulse (for PGE + CD-1012 mixture) shows no spectral features of the first intermediate. Table 2 summarizes the spectral features and lifetimes of these intermediates and their components.

Table 2. Spectral features and the lifetime of intermediates observed for PGE and PGE/CD-1012 by pulse radiolysis.

Transients Observed	CD-1012 Present	Components Present	Absorption Peaks Observed (nm)	Quenched by Oxygen	Observed Lifetimes
1	No	1	300 (sharp), 400 (shoulder), 450–700 (broad)	No	3.6–8.6 μs, 70–90 μs
2	No	2	340 (sharp), 430 (sharp)	Yes No	1, 70 μs, 1–5 μs, 60–70 μs
1	Yes	ND[a]	360 (sharp), 400 (sharp), 500-800 (broad)	ND[a]	ND[a]

[a] Not determined.

5. Conclusions

UV photolysis of Tactix 123 in the presence of photoinitiator CD-1012 (3% by weight) proceeds efficiently to produce mainly a cross-linked insoluble polymer. The first-order reaction rate for the polymerization process ($k_1 = 7.6 \times 10^{-4}\ s^{-1}$) appears to be insensitive to temperature. An activation energy of 61 kJ/mole was determined for the polymerization process.

Kinetics of PGE polymerization by pulse radiolysis has revealed that upon excitation, PGE produces two intermediates that absorb in the UV-Vis region of the spectrum. The first intermediate shows a strong absorption band at 300 nm. The second intermediate that absorbs above 400 nm contains two short-lived components—one sensitive and the other insensitive to oxygen. The rise time of these components is about 2 μs. It appears that decomposition of the oxygen-sensitive component results in the production of additional amounts of first intermediate that absorbs at 300 nm. Based on our kinetic data, we have assigned two plausible structures to these components. The oxygen-sensitive intermediate can form by a PGE radical after abstraction of a hydrogen atom from one of the carbon atoms of the epoxy moiety without ring opening (4 and 4a in Figure 16). The oxygen-insensitive component can form as a zwitterionic species (2 in Figure 16). The components of first intermediate can be assigned to two ketyl radicals, 9 and 9a (Figure 16), which are in equilibrium with their resonance forms, 10 and 10a (Figure 16). All the intermediates produced upon pulse radiolysis of PGE under different reaction conditions (oxygen, nitrogen, and nitrous oxide saturated) seem to derive from the cation radical of PGE. Solvated electrons do not produce any intermediate that absorbs in the UV-Vis region of the spectrum on a 0- to 200-μs time scale.

PGE in the presence of CD-1012 (3%) produces a different set of intermediates with red-shifted absorption. Radiolysis of PGE in the presence of CD-1012 does not proceed to form the first intermediate as seen in direct excitation of PGE. Instead, the second intermediate, which is formed initially, reduces iodonium salt to form an ion pair of PGE/CD-1012. Alternatively, solvated electrons could also reduce iodonium salt to produce an aryl iodide, an aryl radical, and an anion of iodonium salt (Figure 18). Reaction of the aryl radical with PGE produces a PGE radical capable of reducing iodonium salt. Hydrogen abstraction from PGE by iodonium anion produces a strong Brönsted acid, which catalyzes the epoxide ring opening and is followed by the polymerization process. Experiments are currently underway to unravel the reaction pathways that are responsible for the observed polymerization process.

INTENTIONALLY LEFT BLANK.

6. References

1. Seidel, J. R., and D. R. Randell (editors). *Radiation Curing of Polymers.* London: The Royal Society of Chemistry, p. 12, 1987.
2. Garnett, J. L. "Radiation Curing—Twenty Five Years." *Radiation Physics and Chemistry,* vol. 46, p. 925, 1995.
3. Saunders, C. B., V. J. Lopata, W. Kremers, M. Chung, and J. W. Barnard. "Electron and X-ray Curing for Composite Repair." *SAMPE International Symposium,* vol. 40, p. 112, 1995.
4. Janke, C. J., S. J. Havens, G. F. Dorsay, and V. J. Lopata. "Electron Beam Curing of Epoxy Resins by Cationic Polymerization." *SAMPE International Symposium,* vol. 41, p. 196, 1996.
5. Janke, C. J., S. J. Havens, V. J. Lopata, and M. Chung. "Electron Beam Cure of Composites." *SAMPE International Technical Conference,* vol. 28, p. 901, 1996.
6. Goodman, D., L. Brix, G. R. Palmese, and A. Chen. "Composite Curing With High Energy Electron Beams." *SAMPE International Symposium,* vol. 41, p. 207, 1996.
7. Lapin, S. C. "Radiation-Induced Cationic Curing of Vinyl Ether Functionalized Urethane Oligomers." *Polymer Material Science Engineering,* vol 60, p. 233–237, 1989.
8. Crivello, J. V., M. Fan, and D. Bi. "The Electron-Beam Induced Cationic Polymerization of Epoxy Resins." *Journal of Applied Polymer Science,* vol. 44, p. 9, 1992.
9. Crivello, J. V. "UV and Electron Beam-Induced Cationic Polymerization." *Nuclear Instruments and Methods in Physics Research Section B,* vol. 151, p. 8, 1999.
10. Hug, G. L., Y. Wang, C. Schöneich, P.-Y. Jiang, and R. W. Fessenden. "Multiple Time Scales in Pulse Radiolysis: Application to Bromide Solutions and Dipeptides." *Radiation Physics and Chemistry,* vol. 54, no. 6, pp. 559–566, 1999.

INTENTIONALLY LEFT BLANK.

NO. OF COPIES	ORGANIZATION
2	DEFENSE TECHNICAL INFORMATION CENTER DTIC OCA 8725 JOHN J KINGMAN RD STE 0944 FT BELVOIR VA 22060-6218
1	HQDA DAMO FDT 400 ARMY PENTAGON WASHINGTON DC 20310-0460
1	OSD OUSD(A&T)/ODDR&E(R) DR R J TREW 3800 DEFENSE PENTAGON WASHINGTON DC 20301-3800
1	COMMANDING GENERAL US ARMY MATERIEL CMD AMCRDA TF 5001 EISENHOWER AVE ALEXANDRIA VA 22333-0001
1	INST FOR ADVNCD TCHNLGY THE UNIV OF TEXAS AT AUSTIN 3925 W BRAKER LN STE 400 AUSTIN TX 78759-5316
1	US MILITARY ACADEMY MATH SCI CTR EXCELLENCE MADN MATH MAJ HUBER THAYER HALL WEST POINT NY 10996-1786
1	DIRECTOR US ARMY RESEARCH LAB AMSRL D DR D SMITH 2800 POWDER MILL RD ADELPHI MD 20783-1197
1	DIRECTOR US ARMY RESEARCH LAB AMSRL CI AI R 2800 POWDER MILL RD ADELPHI MD 20783-1197

NO. OF COPIES	ORGANIZATION
3	DIRECTOR US ARMY RESEARCH LAB AMSRL CI LL 2800 POWDER MILL RD ADELPHI MD 20783-1197
3	DIRECTOR US ARMY RESEARCH LAB AMSRL CI IS T 2800 POWDER MILL RD ADELPHI MD 20783-1197

ABERDEEN PROVING GROUND

NO. OF COPIES	ORGANIZATION
2	DIR USARL AMSRL CI LP (BLDG 305)

NO. OF COPIES	ORGANIZATION
1	DIRECTOR US ARMY RESEARCH LAB AMSRL CP CA D SNIDER 2800 POWDER MILL RD ADELPHI MD 20783-1197
1	DIRECTOR US ARMY RESEARCH LAB AMSRL CI IS R 2800 POWDER MILL RD ADELPHI MD 20783-1197
3	DIRECTOR US ARMY RESEARCH LAB AMSRL OP SD TL 2800 POWDER MILL RD ADELPHI MD 20783-1197
1	DIRECTOR US ARMY RESEARCH LAB AMSRL CI IS T 2800 POWDER MILL RD ADELPHI MD 20783-1197
1	DPTY ASST SECY FOR R&T SARD TT THE PENTAGON RM 3EA79 WASHINGTON DC 20301-7100
1	COMMANDER US ARMY MATERIEL CMD AMXMI INT 5001 EISENHOWER AVE ALEXANDRIA VA 22333-0001
4	COMMANDER US ARMY ARDEC AMSTA AR CC G PAYNE J GEHBAUER C BAULIEU H OPAT PICATINNY ARSENAL NJ 07806-5000

NO. OF COPIES	ORGANIZATION
2	COMMANDER US ARMY ARDEC AMSTA AR AE WW E BAKER J PEARSON PICATINNY ARSENAL NJ 07806-5000
1	COMMANDER US ARMY ARDEC AMSTA AR TD C SPINELLI PICATINNY ARSENAL NJ 07806-5000
1	COMMANDER US ARMY ARDEC AMSTA AR FSE PICATINNY ARSENAL NJ 07806-5000
6	COMMANDER US ARMY ARDEC AMSTA AR CCH A W ANDREWS S MUSALLI R CARR M LUCIANO E LOGSDEN T LOUZEIRO PICATINNY ARSENAL NJ 07806-5000
1	COMMANDER US ARMY ARDEC AMSTA AR CCH P J LUTZ PICATINNY ARSENAL NJ 07806-5000
1	COMMANDER US ARMY ARDEC AMSTA AR FSF T C LIVECCHIA PICATINNY ARSENAL NJ 07806-5000
1	COMMANDER US ARMY ARDEC AMSTA ASF PICATINNY ARSENAL NJ 07806-5000

NO. OF COPIES	ORGANIZATION
1	COMMANDER US ARMY ARDEC AMSTA AR QAC T C C PATEL PICATINNY ARSENAL NJ 07806-5000
1	COMMANDER US ARMY ARDEC AMSTA AR M D DEMELLA PICATINNY ARSENAL NJ 07806-5000
3	COMMANDER US ARMY ARDEC AMSTA AR FSA A WARNASH B MACHAK M CHIEFA PICATINNY ARSENAL NJ 07806-5000
2	COMMANDER US ARMY ARDEC AMSTA AR FSP G M SCHIKSNIS D CARLUCCI PICATINNY ARSENAL NJ 07806-5000
1	COMMANDER US ARMY ARDEC AMSTA AR FSP A P KISATSKY PICATINNY ARSENAL NJ 07806-5000
2	COMMANDER US ARMY ARDEC AMSTA AR CCH C H CHANIN S CHICO PICATINNY ARSENAL NJ 07806-5000
1	COMMANDER US ARMY ARDEC AMSTA AR QAC T D RIGOGLIOSO PICATINNY ARSENAL NJ 07806-5000

NO. OF COPIES	ORGANIZATION
1	COMMANDER US ARMY ARDEC AMSTA AR WET T SACHAR BLDG 172 PICATINNY ARSENAL NJ 07806-5000
9	COMMANDER US ARMY ARDEC AMSTA AR CCH B P DONADIA F DONLON P VALENTI C KNUTSON G EUSTICE S PATEL G WAGNECZ R SAYER F CHANG PICATINNY ARSENAL NJ 07806-5000
6	COMMANDER US ARMY ARDEC AMSTA AR CCL F PUZYCKI R MCHUGH D CONWAY E JAROSZEWSKI R SCHLENNER M CLUNE PICATINNY ARSENAL NJ 07806-5000
5	PM SADARM SFAE GCSS SD COL B ELLIS M DEVINE W DEMASSI J PRITCHARD S HROWNAK PICATINNY ARSENAL NJ 07806-5000
1	US ARMY ARDEC INTELLIGENCE SPECIALIST AMSTA AR WEL F M GUERRIERE PICATINNY ARSENAL NJ 07806-5000

NO. OF COPIES	ORGANIZATION
2	PEO FIELD ARTILLERY SYS SFAE FAS PM H GOLDMAN T MCWILLIAMS PICATINNY ARSENAL NJ 07806-5000
12	PM TMAS SFAE GSSC TMA R MORRIS C KIMKER D GUZIEWICZ E KOPACZ R ROESER R DARCY R KOWALSKI R MCDANOLDS L D ULISSE C ROLLER J MCGREEN B PATTER PICATINNY ARSENAL NJ 07806-5000
1	COMMANDER US ARMY ARDEC AMSTA AR WEA J BRESCIA PICATINNY ARSENAL NJ 07806-5000
1	COMMANDER US ARMY ARDEC PRODUCTION BASE MODERN ACTY AMSMC PBM K PICATINNY ARSENAL NJ 07806-5000
1	COMMANDER US ARMY TACOM PM ABRAMS SFAE ASM AB 6501 ELEVEN MILE RD WARREN MI 48397-5000
1	COMMANDER US ARMY TACOM AMSTA SF WARREN MI 48397-5000

NO. OF COPIES	ORGANIZATION
3	COMMANDER US ARMY TACOM PM TACTICAL VEHICLES SFAE TVL SFAE TVM SFAE TVH 6501 ELEVEN MILE RD WARREN MI 48397-5000
1	COMMANDER US ARMY TACOM PM BFVS SFAE ASM BV 6501 ELEVEN MILE RD WARREN MI 48397-5000
1	COMMANDER US ARMY TACOM PM AFAS SFAE ASM AF 6501 ELEVEN MILE RD WARREN MI 48397-5000
1	COMMANDER US ARMY TACOM PM RDT&E SFAE GCSS W AB J GODELL 6501 ELEVEN MILE RD WARREN MI 48397-5000
2	COMMANDER US ARMY TACOM PM SURV SYS SFAE ASM SS T DEAN SFAE GCSS W GSI M D COCHRAN 6501 ELEVEN MILE RD WARREN MI 48397-5000
1	US ARMY CERL R LAMPO 2902 NEWMARK DR CHAMPAIGN IL 61822

NO. OF COPIES	ORGANIZATION
1	COMMANDER US ARMY TACOM PM SURVIVABLE SYSTEMS SFAE GCSS W GSI H M RYZYI 6501 ELEVEN MILE RD WARREN MI 48397-5000
1	COMMANDER US ARMY TACOM PM BFVS SFAE GCSS W BV S DAVIS 6501 ELEVEN MILE RD WARREN MI 48397-5000
1	COMMANDER US ARMY TACOM CHIEF ABRAMS TESTING SFAE GCSS W AB QT T KRASKIEWICZ 6501 ELEVEN MILE RD WARREN MI 48397-5000
1	COMMANDER WATERVLIET ARSENAL SMCWV QAE Q B VANINA BLDG 44 WATERVLIET NY 12189-4050
2	TSM ABRAMS ATZK TS S JABURG W MEINSHAUSEN FT KNOX KY 40121
3	ARMOR SCHOOL ATZK TD R BAUEN J BERG A POMEY FT KNOX KY 40121

NO. OF COPIES	ORGANIZATION
14	COMMANDER US ARMY TACOM AMSTA TR R R MCCLELLAND D THOMAS J BENNETT D HANSEN AMSTA JSK S GOODMAN J FLORENCE K IYER D TEMPLETON A SCHUMACHER AMSTA TR D D OSTBERG L HINOJOSA B RAJU AMSTA CS SF H HUTCHINSON F SCHWARZ WARREN MI 48397-5000
14	BENET LABORATORIES AMSTA AR CCB R FISCELLA M SOJA E KATHE M SCAVULO G SPENCER P WHEELER S KRUPSKI J VASILAKIS G FRIAR R HASENBEIN AMSTA CCB R S SOPOK E HYLAND D CRAYON R DILLON WATERVLIET NY 12189-4050
2	HQ IOC TANK AMMUNITION TEAM AMSIO SMT R CRAWFORD W HARRIS ROCK ISLAND IL 61299-6000

NO. OF COPIES	ORGANIZATION
2	COMMANDER US ARMY AMCOM AVIATION APPLIED TECH DIR J SCHUCK FT EUSTIS VA 23604-5577
1	DIRECTOR US ARMY AMCOM SFAE AV RAM TV D CALDWELL BLDG 5300 REDSTONE ARSENAL AL 35898
2	US ARMY CORPS OF ENGINEERS CERD C T LIU CEW ET T TAN 20 MASS AVE NW WASHINGTON DC 20314
1	SYSTEM MANAGER ABRAMS ATZK TS LTC J H NUNN BLDG 1002 RM 110 FT KNOX KY 40121
2	USA SBCCOM MATERIAL SCIENCE TEAM AMSSB RSS J HERBERT M SENNETT KANSAS ST NATICK MA 01760-5057
2	OFC OF NAVAL RESEARCH D SIEGEL CODE 351 J KELLY 800 N QUINCY ST ARLINGTON VA 22217-5660
1	NAVAL SURFACE WARFARE CTR DAHLGREN DIV CODE G06 DAHLGREN VA 22448
1	NAVAL SURFACE WARFARE CTR TECH LIBRARY CODE 323 17320 DAHLGREN RD DAHLGREN VA 22448

NO. OF COPIES	ORGANIZATION
1	NAVAL SURFACE WARFARE CTR CRANE DIVISION M JOHNSON CODE 20H4 LOUISVILLE KY 40214-5245
2	NAVAL SURFACE WARFARE CTR U SORATHIA C WILLIAMS CD 6551 9500 MACARTHUR BLVD WEST BETHESDA MD 20817
2	COMMANDER NAVAL SURFACE WARFARE CTR CARDEROCK DIVISION R PETERSON CODE 2020 M CRITCHFIELD CODE 1730 BETHESDA MD 20084
8	US ARMY SBCCOM SOLDIER SYSTEMS CENTER BALLISTICS TEAM J WARD W ZUKAS P CUNNIFF J SONG MARINE CORPS TEAM J MACKIEWICZ BUS AREA ADVOCACY TEAM W HASKELL AMSSB RCP SS W NYKVIST S BEAUDOIN KANSAS ST NATICK MA 01760-5019
9	US ARMY RESEARCH OFC A CROWSON J CHANDRA H EVERETT J PRATER R SINGLETON G ANDERSON D STEPP D KISEROW J CHANG PO BOX 12211 RESEARCH TRIANGLE PARK NC 27709-2211

NO. OF COPIES	ORGANIZATION
8	NAVAL SURFACE WARFARE CTR J FRANCIS CODE G30 D WILSON CODE G32 R D COOPER CODE G32 J FRAYSSE CODE G33 E ROWE CODE G33 T DURAN CODE G33 L DE SIMONE CODE G33 R HUBBARD CODE G33 DAHLGREN VA 22448
1	NAVAL SEA SYSTEMS CMD D LIESE 2531 JEFFERSON DAVIS HWY ARLINGTON VA 22242-5160
1	NAVAL SURFACE WARFARE CTR M LACY CODE B02 17320 DAHLGREN RD DAHLGREN VA 22448
2	NAVAL SURFACE WARFARE CTR CARDEROCK DIVISION R CRANE CODE 2802 C WILLIAMS CODE 6553 3A LEGGETT CIR BETHESDA MD 20054-5000
1	EXPEDITIONARY WARFARE DIV N85 F SHOUP 2000 NAVY PENTAGON WASHINGTON DC 20350-2000
1	AFRL MLBC M FORTE 2941 P ST RM 136 WRIGHT PATTERSON AFB OH 45433-7750
1	AFRL MLSS R THOMSON 2179 12TH ST RM 122 WRIGHT PATTERSON AFB OH 45433-7718
1	WATERWAYS EXPERIMENT D SCOTT 3909 HALLS FERRY RD SC C VICKSBURG MS 39180

NO. OF COPIES	ORGANIZATION
2	AFRL F ABRAMS J BROWN BLDG 653 2977 P ST STE 6 WRIGHT PATTERSON AFB OH 45433-7739
5	DIRECTOR LLNL R CHRISTENSEN S DETERESA F MAGNESS M FINGER MS 313 M MURPHY L 282 PO BOX 808 LIVERMORE CA 94550
1	AFRL MLS OL L COULTER 7278 4TH ST BLDG 100 BAY D HILL AFB UT 84056-5205
1	OSD JOINT CCD TEST FORCE OSD JCCD R WILLIAMS 3909 HALLS FERRY RD VICKSBURG MS 29180-6199
3	DARPA M VANFOSSEN S WAX L CHRISTODOULOU 3701 N FAIRFAX DR ARLINGTON VA 22203-1714
2	SERDP PROGRAM OFC PM P2 C PELLERIN B SMITH 901 N STUART ST STE 303 ARLINGTON VA 22203

NO. OF COPIES	ORGANIZATION
1	FAA MIL HDBK 17 CHAIR L ILCEWICZ 1601 LIND AVE SW ANM 115N RESTON VA 98055
1	US DEPT OF ENERGY OFC OF ENVIRONMENTAL MANAGEMENT P RITZCOVAN 19901 GERMANTOWN RD GERMANTOWN MD 20874-1928
1	DIRECTOR LLNL F ADDESSIO MS B216 PO BOX 1633 LOS ALAMOS NM 87545
1	OAK RIDGE NATIONAL LABORATORY R M DAVIS PO BOX 2008 OAK RIDGE TN 37831-6195
1	OAK RIDGE NATIONAL LABORATORY C EBERLE MS 8048 PO BOX 2008 OAK RIDGE TN 37831
1	OAK RIDGE NATIONAL LABORATORY C D WARREN MS 8039 PO BOX 2008 OAK RIDGE TN 37831
5	NIST J DUNKERS M VANLANDINGHAM MS 8621 J CHIN MS 8621 J MARTIN MS 8621 D DUTHINH MS 8611 100 BUREAU DR GAITHERSBURG MD 20899
3	HYDROGEOLOGIC INC SERDP ESTCP SPT OFC S WALSH 1155 HERNDON PKWY STE 900 HERNDON VA 20170

NO. OF COPIES	ORGANIZATION
3	NASA LANGLEY RSCH CTR AMSRL VS W ELBER MS 266 F BARTLETT JR MS 266 G FARLEY MS 266 HAMPTON VA 23681-0001
1	NASA LANGLEY RSCH CTR T GATES MS 188E HAMPTON VA 23661-3400
1	FHWA E MUNLEY 6300 GEORGETOWN PIKE MCLEAN VA 22101
1	CYTEC FIBERITE R MAYHEW 1300 REVOLUTION ST HAVRE DE GRACE MD 21078
2	3TEX CORPORATION A BOGDANOVICH J SINGLETARY 109 MACKENAN DR CARY NC 27511
1	3M CORPORATION J SKILDUM 3M CENTER BLDG 60 IN 01 ST PAUL MN 55144-1000
1	COMPOSITE MATERIALS INC D SHORTT 19105 63 AVE NE PO BOX 25 ARLINGTON WA 98223
1	COMPOSITE MATERIALS INC R HOLLAND 11 JEWEL CT ORINDA CA 94563
1	COMPOSITE MATERIALS INC C RILEY 14530 S ANSON AVE SANTA FE SPRINGS CA 90670

NO. OF COPIES	ORGANIZATION
2	SIMULA J COLTMAN R HUYETT 10016 S 51ST ST PHOENIX AZ 85044
2	PROTECTION MATERIALS INC M MILLER F CRILLEY 14000 NW 58 CT MIAMI LAKES FL 33014
3	FOSTER MILLER J J GASSNER M ROYLANCE W ZUKAS 195 BEAR HILL RD WALTHAM MA 02354-1196
2	TEXTRON SYSTEMS T FOLTZ M TREASURE 1449 MIDDLESEX ST LOWELL MA 01851
2	MILLIKEN RSCH CORP H KUHN M MACLEOD PO BOX 1926 SPARTANBURG SC 29303
1	CONNEAUGHT INDUSTRIES INC J SANTOS PO BOX 1425 COVENTRY RI 02816
1	ARMTEC DEFENSE PRODUCTS S DYER 85 901 AVE 53 PO BOX 848 COACHELLA CA 92236
1	NATIONAL COMPOSITE CENTER T CORDELL 2000 COMPOSITE DR KETTERING OH 45420

NO. OF COPIES	ORGANIZATION
3	PACIFIC NORTHWEST LAB M SMITH G VAN ARSDALE R SHIPPELL PO BOX 999 RICHLAND WA 99352
2	AMOCO PERFORMANCE PRODUCTS M MICHNO JR J BANISAUKAS 4500 MCGINNIS FERRY RD ALPHARETTA GA 30202-3944
8	ALLIANT TECHSYSTEMS INC C CANDLAND MN11 2830 C AAKHUS MN11 2830 B SEE MN11 2439 N VLAHAKUS MN11 2145 R DOHRN MN11 2830 S HAGLUND MN11 2439 M HISSONG MN11 2830 D KAMDAR MN11 2830 600 SECOND ST NE HOPKINS MN 55343-8367
1	CUSTOM ANALYTICAL ENG SYS INC A ALEXANDER 13000 TENSOR LANE NE FLINTSTONE MD 21530
3	ALLIANT TECHSYSTEMS INC J CONDON E LYNAM J GERHARD WV01 16 STATE RT 956 PO BOX 210 ROCKET CENTER WV 26726-0210
1	OFC DEPUTY UNDER SEC DEFNS J THOMPSON 1745 JEFFERSON DAVIS HWY CRYSTAL SQ 4 STE 501 ARLINGTON VA 22202
1	PROJECTILE TECHNOLOGY INC 515 GILES ST HAVRE DE GRACE MD 21078

NO. OF COPIES	ORGANIZATION
5	AEROJET GEN CORP D PILLASCH T COULTER C FLYNN D RUBAREZUL M GREINER 1100 WEST HOLLYVALE ST AZUSA CA 91702-0296
3	HEXCEL INC R BOE PO BOX 18748 SALT LAKE CITY UT 84118
1	ZERNOW TECHNICAL SERVICES L ZERNOW 425 W BONITA AVE STE 208 SAN DIMAS CA 91773
1	GKN AEROSPACE D OLDS 15 STERLING DR WALLINGFORD CT 06492
5	SIKORSKY AIRCRAFT G JACARUSO T CARSTENSAN B KAY S GARBO MS S330A J ADELMANN 6900 MAIN ST PO BOX 9729 STRATFORD CT 06497-9729
1	PRATT & WHITNEY C WATSON 400 MAIN ST MS 114 37 EAST HARTFORD CT 06108
1	AEROSPACE CORP G HAWKINS M4 945 2350 E EL SEGUNDO BLVD EL SEGUNDO CA 90245
2	CYTEC FIBERITE M LIN W WEB 1440 N KRAEMER BLVD ANAHEIM CA 92806

NO. OF COPIES	ORGANIZATION
1	UDLP G THOMAS PO BOX 58123 SANTA CLARA CA 95052
2	BOEING DFNSE & SPACE GP W HAMMOND S 4X55 J RUSSELL S 4X55 PO BOX 3707 SEATTLE WA 98124-2207
1	LOCKHEED MARTIN SKUNK WORKS D FORTNEY 1011 LOCKHEED WAY PALMDALE CA 93599-2502
1	MATERIALS SCIENCES CORP G FLANAGAN 500 OFC CENTER DR STE 250 FT WASHINGTON PA 19034
2	UNIV OF DAYTON RESEARCH INST R Y KIM A K ROY 300 COLLEGE PARK AVE DAYTON OH 45469-0168
1	UMASS LOWELL PLASTICS DEPT N SCHOTT 1 UNIVERSITY AVE LOWELL MA 01854
1	UNIV OF MAINE ADV STR & COMP LAB R LOPEZ ANIDO 5793 AEWC BLDG ORONO ME 04469-5793
1	JOHNS HOPKINS UNIV APPLIED PHYSICS LAB P WIENHOLD 11100 JOHNS HOPKINS RD LAUREL MD 20723-6099

NO. OF COPIES	ORGANIZATION
1	UNIV OF DAYTON J M WHITNEY COLLEGE PARK AVE DAYTON OH 45469-0240
2	UNIV OF DELAWARE CTR FOR COMPOSITE MTRLS J GILLESPIE S YARLAGADDA 201 SPENCER LABORATORY NEWARK DE 19716
1	DEPT OF MATERIALS SCIENCE & ENGINEERING UNIVERSITY OF ILLINOIS AT URBANA CHAMPAIGN J ECONOMY 1304 WEST GREEN ST 115B URBANA IL 61801
1	UNIV OF MARYLAND DEPT OF AEROSPACE ENGNRNG A J VIZZINI COLLEGE PARK MD 20742
2	DREXEL UNIV A S D WANG G PALMESE 32ND & CHESTNUT ST PHILADELPHIA PA 19104
1	SOUTHWEST RSCH INST ENGR & MATL SCIENCES DIV J RIEGEL 6220 CULEBRA RD PO DRAWER 28510 SAN ANTONIO TX 78228-0510
1	UNIV OF TENNESSEE AT KNOXVILLE K KIT 434 DOUGHERTY ENGR BLDG KNOXVILLE TN 37996-2200
2	YLA INCORPORATED S DUGGAN R RAMERIZ 2970 BAY VISTA COURT BENICIA CA 94510

NO. OF COPIES	ORGANIZATION
2	BOEING M WILENSKI J BURGESS PO BOX 3999 MC73 09 SEATTLE WA 98124-2499
1	E BEAM SERVICE INC M STERN 32 MELRICH ROAD CRANBURY NJ 08512
2	UCB CHEMICALS CORP M JOHNSON S WILLIAMSON 2000 LAKE PARK DRIVE SMYRNA GA 30080
1	APPLIED POLERAMIC INC R MOULTON 850 TEAM DRIVE BENICIA CA 94510-1249
2	SCIENCE RESEARCH LAB C BYRNE 15 WARD STREET SOMERVILLE MA 02143
3	SERDP AND ESTCP PRGM OFC B SMITH C PELLERIN J MARQUSEE 901 N STUART STREET SUITE 303 ARLINGTON VA 22203
1	LOCKHEED MARTIN TACTICAL AIRCRAFT SYSTEMS P KIRN 1 LOCKHEED BLVD PO BOX 748 MS 2852 FORT WORTH TX 76101-0748
1	LOCKHEED MARTIN SPACE SYSTEMS COMPANY J CHOI 13800 OLD GENTILLY RD NEW ORLEANS LA 70129

NO. OF COPIES	ORGANIZATION
1	MICHIGAN STATE UNIVERSITY COMPOSITES CENTER L DRZAL 2100 ENGR BLDG EAST LANSING MI 48824-1226
1	ADHERENT TECHNOLOGIES INC A HOYT 11208 COCHITI ST ALBUQUERQUE NM 87123
2	ORNL R DABESTANI MS 6100 I IVANOV MS 6100 BLDG 4500S PO BOX 2008 OAK RIDGE TN 37831
1	ORNL C JANKE MS 8048 BLDG 4500S PO BOX 2008 OAK RIDGE TN 37831
1	DIRECTOR US ARMY RESEARCH LAB AMSRL WM MB A FRYDMAN 2800 POWDER MILL RD ADELPHI MD 20783-1197
1	DIRECTOR US ARMY RESEARCH LAB AMSRL SS SD H WALLACE 2800 POWDER MILL RD ADELPHI MD 20783-1197
2	DIRECTOR US ARMY RESEARCH LAB AMSRL SE DS R ATKINSON R REYZER 2800 POWDER MILL RD ADELPHI MD 20783-1197

ABERDEEN PROVING GROUND

1	US ARMY MATERIEL SYSTEMS ANALYSIS ACTIVITY P DIETZ 392 HOPKINS RD AMXSY TD APG MD 21005-5071
1	DIRECTOR US ARMY RESEARCH LAB AMSRL OP AP L APG MD 21005-5066
88	DIR USARL AMSRL CI AMSRL CI S A MARK AMSRL CS IO FI M ADAMSON AMSRL SL BA AMSRL SL BL D BELY R HENRY AMSRL SL BG AMSRL SL I AMSRL WM J SMITH AMSRL WM B A HORST AMSRL WM BA D LYON AMSRL WM BC J NEWILL P PLOSTINS S WILKERSON A ZIELINSKI AMSRL WM BD R FIFER B FORCH R PESCE RODRIGUEZ B RICE AMSRL WM BE C LEVERITT AMSRL WM BF J LACETERA AMSRL WM BR J BORNSTEIN C SHOEMAKER AMSRL WM M G HAGNAUER

NO. OF
COPIES ORGANIZATION

ABERDEEN PROVING GROUND (CONT)

J MCCAULEY
D VIECHNICKI
AMSRL WM MA
L GHIORSE
S MCKNIGHT
AMSRL WM MB
J BENDER
T BOGETTI
R BOSSOLI
K BOYD
L BURTON
S CORNELISON
P DEHMER
R DOOLEY
W DRYSDALE
B FINK
G GAZONAS
S GHIORSE
D GRANVILLE
D HENRY
D HOPKINS
C HOPPEL
R KASTE
M KLUSEWITZ
M LEADORE
R LIEB
E RIGAS
J SANDS
D SPAGNUOLO
W SPURGEON
J TZENG
E WETZEL
AMRSL WM MC
J BEATTY
E CHIN
J LASALVIA
J MONTGOMERY
J WELLS
A WERECZCAK
AMSRL WM MD
W ROY
S WALSH
AMSRL WM T
W BRUCHEY
M BURKINS
B BURNS
M ZOLTOSKI

ABERDEEN PROVING GROUND (CONT)

AMSRL WM TA
W GILLICH
T HAVEL
J RUNYEON
E HORWATH
B GOOCH
M NORMANDIA
AMRSL WM TB
D KOOKER
P BAKER
AMSRL WM TC
R COATES
AMSRL WM TD
M BOTELER
D DANDEKAR
A DAS GUPTA
F GREGORY
T HADUCH
T MOYNIHAN
M RAFTENBERG
T WEERASOORIYA
AMSRL WM TE
A NIILER
J POWELL

NO. OF COPIES	ORGANIZATION
1	ACSION INDUSTRIES V LOPATA PO BOX 429 PINAWA MB R0E 1L0 CANADA
1	NATIONAL RESEARCH COUNCIL CANADA A JOHNSTON 1500 MONTREAL ROAD BLDG M 3 OTTAWA ON K1A 0R6 CANADA
1	NATIONAL RESEARCH COUNCIL CANADA K COLE 75 DE MORTAGNE BLVD BOUCHERVILLE QUEBEC J4B 6Y4

REPORT DOCUMENTATION PAGE

Form Approved
OMB No. 0704-0188

1. AGENCY USE ONLY *(Leave blank)*	2. REPORT DATE	3. REPORT TYPE AND DATES COVERED
	April 2002	Final, November 2000–March 2001

4. TITLE AND SUBTITLE
Cationic Polymerization (Cure Kinetics) of Model Expoxide Systems

5. FUNDING NUMBERS
622618.H80

6. AUTHOR(S)
Reza Dabestani,* Illia N. Ivanov* and James M. Sands

7. PERFORMING ORGANIZATION NAME(S) AND ADDRESS(ES)
U.S. Army Research Laboratory
ATTN: AMSRL-WM-MB
Aberdeen Proving Ground, MD 21005-5069

8. PERFORMING ORGANIZATION REPORT NUMBER
ARL-TR-2714

9. SPONSORING/MONITORING AGENCY NAMES(S) AND ADDRESS(ES)
SERDP-PP1109 Customer Program
901 N. Stuart Street
Arlington, VA 22203

10.SPONSORING/MONITORING AGENCY REPORT NUMBER

11. SUPPLEMENTARY NOTES
*Chemical Sciences Division, Oak Ridge National Laboratory, P.O. Box 2008, Oak Ridge, TN 37831-6100

12a. DISTRIBUTION/AVAILABILITY STATEMENT
Approved for public release; distribution is unlimited.

12b. DISTRIBUTION CODE

13. ABSTRACT *(Maximum 200 words)*

Cationic polymerization of epoxy resins can be induced by ultraviolet (UV) or electron beam (E-beam) radiation and proceeds very efficiently in the presence of an appropriate photoinitiator. Although good thermal properties have been obtained for some E-beam cured epoxy resins, other important mechanical properties, such as interlaminar shear strength, fracture toughness, and compression are poor and do not meet aerospace manufacturers materials standards. We have initiated a comprehensive study to investigate the cure kinetics and mechanisms of UV and E-beam cured cationic polymerization of two epoxide-terminated resins (phenyl glycidyl ether (PGE), a monofunctional model compound, and Tactix 123, a difunctional structural resin) cured using a mixed triaryl iodonium hexafluoroantimonate salt (Sartomer's CD-1012) photoinitiator. The objective of this study was to demonstrate that identical reaction conditions and kinetic parameters (e.g., radiation dose, initiator concentration, and reaction temperature) control the physical and chemical properties of final polymeric products, regardless of initiation by UV or E-beam radiation. Additionally, the identification of key parameters that give rise to improved thermal and mechanical properties in E-beam processed resins is sought. Fast kinetic spectroscopy, coupled with high-performance liquid chromatography, was used to elucidate the polymerization mechanism and to identify the reactive intermediates, or molecules, involved in the cure process.

14. SUBJECT TERMS
electron beam cure, epoxides, PGE, mechanisms, cationic initiator

15. NUMBER OF PAGES
45

16. PRICE CODE

17. SECURITY CLASSIFICATION OF REPORT	18. SECURITY CLASSIFICATION OF THIS PAGE	19. SECURITY CLASSIFICATION OF ABSTRACT	20. LIMITATION OF ABSTRACT
UNCLASSIFIED	UNCLASSIFIED	UNCLASSIFIED	UL

NSN 7540-01-280-5500

Standard Form 298 (Rev. 2-89)
Prescribed by ANSI Std. 239-18 298-102

INTENTIONALLY LEFT BLANK.